

# Adaptive iterative learning control for vibration of flexural rectangular plate

Jingyu Yang\*, Guoping Chen\*\*

\*Nanjing University of Aeronautics and Astronautics, 210016 Nanjing, China, E-mail: jingyu220@163.com

\*\*Nanjing University of Aeronautics and Astronautics, 210016 Nanjing, China, E-mail: gpchen@nuaa.edu

crossref <http://dx.doi.org/10.5755/j01.mech.17.5.724>

## 1. Introduction

The adaptive vibration control (AVC) problem of flexible plate structures has attracted considerable attention during the last two decades. Many researchers proposed different control strategies for the purpose of AVC of flexible plate structures. Hu et al [1] applied LMI (Linear Matrix Inequality)-based  $H_\infty$  robust control for AVC of a flexible plate structure. They used specific transformations of Lyapunov variable with appropriate linearizing transformations of the controller variables, which give rise to a tractable and practical LMI formulation of the vibration control problem. Based on LMI, a  $H_\infty$  output feedback controller was designed to suppress the low-frequency vibrations caused by external disturbances. The simulation results showed that the proposed robust active control method is efficient for active vibration suppression. Other research on the effectiveness of the robust  $H_\infty$  control for AVC of the flexible structures has been addressed in [2-4].

Based on the previously outlined literature, there is no published report in which the adaptive iterative learning MIMO control is used for the purpose of intelligent AVC of a flexible rectangular plate system. In this research, an adaptive iterative learning MIMO control strategy is applied to the problem of AVC of a rectangular flexible rectangular plate. First, the flexible rectangular plate system is modeled using the FEM method and new modeling method. Then, the validity of the obtained new model is investigated by comparing the plate natural frequencies, mode shape, static analysis and forced vibration response analysis predicted by the finite element model with the calculated values obtained from new model. After validating the model, adaptive iterative learning MIMO controller is applied to the plate dynamics via the MATLAB/Simulink platform. The algorithms were then coded in MATLAB to evaluate the performance of the control system. Disturbances were employed to excite the plate system at different excitation points and the controller ability to attenuate the vibration of observation point was investigated. The simulation results clearly demonstrate an effective vibration suppression capability that can be achieved using adaptive iterative learning MIMO controller.

## 2. Modelling of flexible rectangular plate system

Cartesian coordinate system  $(x, y, z)$  is introduced, consider a thin flexible rectangular plate of length  $a$  along  $x$ -axis, width  $b$  along  $y$ -axis and thickness  $h$  along  $z$ -axis. This condition is illustrated in Fig. 1.

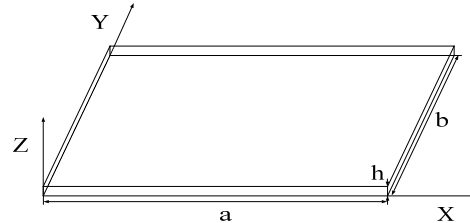


Fig. 1 A flexible rectangular plate

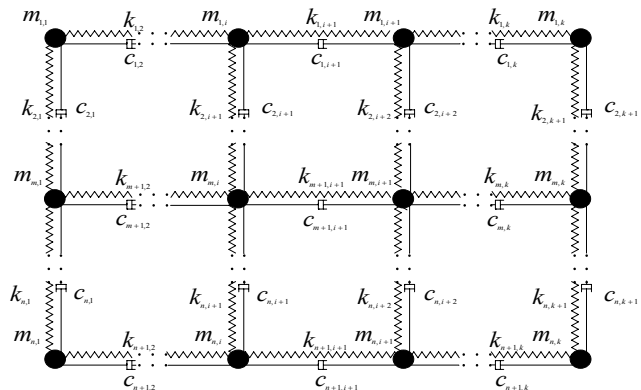


Fig. 2 A discrete flexible rectangular plate

The quality and flexibility of plate structure is a continuous distribution, the system has an infinite number of degrees of freedom. To simplify the research and facilitate the calculation, construct spring-mass system and make the system discrete, the system is simplified as multi DOF vibration system. After the process of discrete, the flexible rectangular plate is shown in Fig. 2. Where  $m_{ij}$  ( $i = 1, 2, \dots, n; j = 1, 2, \dots, k$ ) are masses;  $k_{s,t}$  ( $s = 1, 2, \dots, n+1; t = 1, 2, \dots, k+1$ ) are stiffness coefficients;  $c_{r,p}$  ( $r = 1, 2, \dots, n+1; p = 1, 2, \dots, k+1$ ) are damping coefficients.

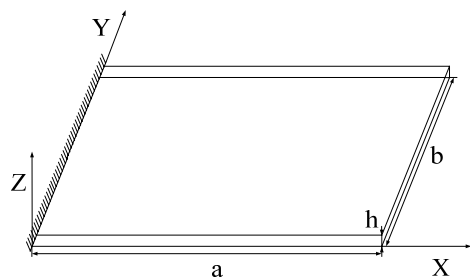


Fig. 3 A flexible cantilever plate

Considering the boundary conditions, take the modeling of cantilever flexible rectangular plate as an example so as to elaborate new flexible rectangular plate modeling method. Consider a thin cantilever flexible rec-

tangular plate of length  $a$  along x-axis, width  $b$  along y-axis and thickness  $h$  along z-axis. This condition is illustrated in Fig. 3. After the process of discrete, the cantilever flexible rectangular plate is shown in Fig. 4. Where  $m_{ij}$  ( $i=1,2,3p$ ;  $j=1,2,3$ ) are masses;  $k_{s,t}$  ( $s=1,2,3,4,5$ ;  $t=1,2,3$ ) are stiffness coefficients;  $c_{r,p}$  ( $r=1,2,3,4,5$ ;  $p=1,2,3$ ) are damping coefficients.

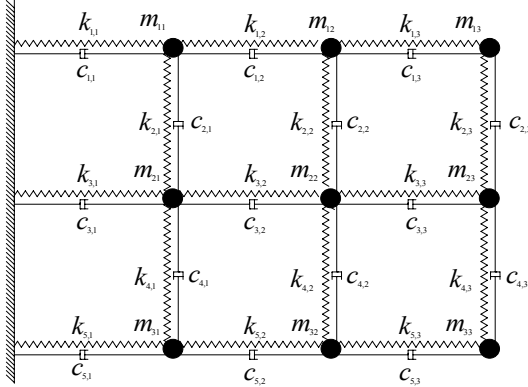


Fig. 4 A discrete flexible cantilever plate

$F_{11}$  is a concentrated force which is applied to  $m_{11}$ ,  $\theta$  is generalized coordinate,  $L$  is the length between the adjacent mass;  $\nabla L$  is the variable value of  $L$ ;  $y$  is the elastic displacement of mass. This condition is illustrated in Fig. 5.

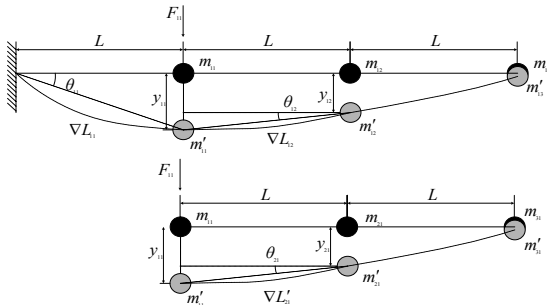


Fig. 5 Dynamic analysis of deformed plate

$$\left. \begin{aligned} \sin \theta_{11} &= \frac{y_{11}}{L + \Delta L_{11}} = \frac{\dot{y}_{11}}{\dot{L} + \Delta \dot{L}_{11}} \\ \sin \theta_{12} &= \frac{y_{11} - y_{12}}{L + \Delta L_{12}} = \frac{\dot{y}_{11} - \dot{y}_{12}}{\dot{L} + \Delta \dot{L}_{12}} \\ \sin \theta_{21} &= \frac{y_{11} - y_{21}}{L + \Delta L_{21}} = \frac{\dot{y}_{11} - \dot{y}_{21}}{\dot{L} + \Delta \dot{L}_{21}} \end{aligned} \right\} (1)$$

$$\Delta L_{11} \ll L; \Delta L_{12} \ll L; \Delta L_{21} \ll L; \dot{L} = 0 \quad (2)$$

$$\left. \begin{aligned} \sin \theta_{11} &= \frac{y_{11}}{L} = \frac{\dot{y}_{11}}{\Delta \dot{L}_{11}}; \sin \theta_{12} = \frac{y_{11} - y_{12}}{L} = \frac{\dot{y}_{11} - \dot{y}_{12}}{\Delta \dot{L}_{12}} \\ \sin \theta_{21} &= \frac{y_{11} - y_{21}}{L} = \frac{\dot{y}_{11} - \dot{y}_{21}}{\Delta \dot{L}_{21}} \end{aligned} \right\} (3)$$

Letting

$$k'_{11} = (k_{11} + k_{12} + k_{21})/3; k'_{12} = (k_{11} + k_{22} + k_{13})/3 \quad (4)$$

$$k'_{13} = (k_{12} + k_{23})/2; k'_{21} = (k_{21} + k_{22} + k_{11} + k_{31})/4 \quad (5)$$

$$k'_{22} = (k_{21} + k_{12} + k_{23} + k_{32})/4; k'_{23} = (k_{22} + k_{13} + k_{33})/3 \quad (6)$$

$$k'_{31} = (k_{31} + k_{21} + k_{32})/3; k'_{32} = (k_{31} + k_{22} + k_{33})/3 \quad (7)$$

$$k'_{33} = (k_{32} + k_{23})/2 \quad (8)$$

Supposed

$$k'_{11} \frac{\nabla L_{11}}{L} \approx k'_{11} \frac{\nabla L_{12}}{L} \approx k'_{11} \frac{\nabla L'_{21}}{L} \approx k'_{11} \frac{\nabla L_1}{L} \quad (9)$$

$$k'_{12} \frac{\nabla L_{11}}{L} \approx k'_{12} \frac{\nabla L_{22}}{L} \approx k'_{12} \frac{\nabla L'_{13}}{L} \approx k'_{12} \frac{\nabla L_2}{L} \quad (10)$$

$$k'_{13} \frac{\nabla L_{12}}{L} \approx k'_{13} \frac{\nabla L_{23}}{L} \approx k'_{13} \frac{\nabla L_3}{L} \quad (11)$$

$$k'_{21} \frac{\nabla L_{21}}{L} \approx k'_{21} \frac{\nabla L_{22}}{L} \approx k'_{21} \frac{\nabla L'_{11}}{L} \approx k'_{21} \frac{\nabla L'_{31}}{L} \approx k'_{21} \frac{\nabla L_4}{L} \quad (12)$$

$$k'_{22} \frac{\nabla L_{21}}{L} \approx k'_{22} \frac{\nabla L_{12}}{L} \approx k'_{22} \frac{\nabla L'_{23}}{L} \approx k'_{22} \frac{\nabla L'_{32}}{L} \approx k'_{22} \frac{\nabla L_5}{L} \quad (13)$$

$$k'_{23} \frac{\nabla L_{22}}{L} \approx k'_{23} \frac{\nabla L_{13}}{L} \approx k'_{23} \frac{\nabla L'_{33}}{L} \approx k'_{23} \frac{\nabla L_6}{L} \quad (14)$$

$$k'_{31} \frac{\nabla L_{31}}{L} \approx k'_{31} \frac{\nabla L_{21}}{L} \approx k'_{31} \frac{\nabla L'_{32}}{L} \approx k'_{31} \frac{\nabla L_7}{L} \quad (15)$$

$$k'_{32} \frac{\nabla L_{31}}{L} \approx k'_{32} \frac{\nabla L_{22}}{L} \approx k'_{32} \frac{\nabla L'_{33}}{L} \approx k'_{32} \frac{\nabla L_8}{L} \quad (16)$$

$$k'_{33} \frac{\nabla L_{32}}{L} \approx k'_{33} \frac{\nabla L_{23}}{L} \approx k'_{33} \frac{\nabla L_3}{L} \quad (17)$$

Letting

$$k'_{11} \frac{\nabla L_1}{L} \approx K_{11}; k'_{12} \frac{\nabla L_2}{L} \approx K_{12}; k'_{13} \frac{\nabla L_3}{L} \approx K_{13} \quad (18)$$

$$k'_{21} \frac{\nabla L_4}{L} \approx K_{21}; k'_{22} \frac{\nabla L_5}{L} \approx K_{22}; k'_{23} \frac{\nabla L_6}{L} \approx K_{23} \quad (19)$$

$$k'_{31} \frac{\nabla L_7}{L} \approx K_{31}; k'_{32} \frac{\nabla L_8}{L} \approx K_{32}; k'_{33} \frac{\nabla L_9}{L} \approx K_{33} \quad (20)$$

$$c'_{11} = C_{11}; c'_{13} = C_{13}; c'_{22} = C_{22} \quad (21)$$

$$c'_{23} = C_{23}; c'_{31} = C_{31}; c'_{32} = C_{32}; c'_{33} = C_{33} \quad (22)$$

We now apply Newton's second law of motion to the mass  $m_{ij} = m$   $i, j = 1, 2, 3, \dots, 7$ , we have

$$M_{11} \ddot{y}_{11} + C_{11} [3\dot{y}_{11} - \dot{y}_{12} - \dot{y}_{21}] + K_{11} [3y_{11} - y_{12} - y_{21}] = F_{11} \quad (23)$$

$$M_{12} \ddot{y}_{12} + C_{12} [3\dot{y}_{11} - \dot{y}_{12} - \dot{y}_{21}] + K_{12} [3y_{12} - y_{13} - y_{22} - y_{11}] = F_{12} \quad (24)$$

$$M_{13} \ddot{y}_{13} + C_{13} [3\dot{y}_{11} - \dot{y}_{12} - \dot{y}_{21}] + K_{13} [2y_{13} - y_{12} - y_{23}] = F_{13} \quad (25)$$

$$M_{21} \ddot{y}_{21} + C_{21} [3\dot{y}_{11} - \dot{y}_{12} - \dot{y}_{21}] + K_{21} [4y_{21} - y_{11} - y_{31} - y_{22}] = F_{21} \quad (26)$$

$$M_{22}\ddot{y}_{22} + C_{22}[3\dot{y}_{11} - \dot{y}_{12} - \dot{y}_{21}] + K_{22}[4y_{22} - y_{21} - y_{12} - y_{32}] = F_{22} \tag{27}$$

$$M_{23}\ddot{y}_{23} + C_{23}[3\dot{y}_{11} - \dot{y}_{12} - \dot{y}_{21}] + K_{23}[3y_{23} - y_{13} - y_{33} - y_{22}] = F_{23} \tag{28}$$

$$M_{31}\ddot{y}_{31} + C_{31}[3\dot{y}_{11} - \dot{y}_{12} - \dot{y}_{21}] + K_{31}[3y_{31} - y_{32} - y_{21}] = F_{31} \tag{29}$$

$$M_{32}\ddot{y}_{32} + C_{32}[3\dot{y}_{11} - \dot{y}_{12} - \dot{y}_{21}] + K_{32}[3y_{32} - y_{33} - y_{22} - y_{31}] = F_{32} \tag{30}$$

$$M_{33}\ddot{y}_{33} + C_{33}[3\dot{y}_{11} - \dot{y}_{12} - \dot{y}_{21}] + K_{33}[2y_{33} - y_{32} - y_{23}] = F_{33} \tag{31}$$

As a convention, we denote a dot as a first derivative with respect to time (i.e.,  $\dot{y} = dx / dt$ ), and a double dot as a second derivative with respect to time (i.e.,  $\ddot{y} = d^2 y / dt^2$ ). Let  $n_d$  be a number of degrees of freedom of the system (linearly independent coordinates describing the finite-dimensional structure), let  $r$  be a number of outputs, and let  $s$  be a number of inputs. A flexible structure in nodal coordinates is represented by the following second-order matrix differential equation

$$[M][\ddot{Y}] + [P][\dot{Y}] + [K][Y] = [L][F] \tag{32}$$

In this equation  $X$  is the  $n_d \times 1$  nodal displacement

vector;  $\dot{Y}$  is the  $n_d \times 1$  nodal velocity vector;  $\ddot{Y}$  is the  $n_d \times 1$  nodal acceleration vector;  $F$  is the  $s \times 1$  input vector;  $[M]$  is the mass matrix,  $n_d \times n_d$ ;  $[P]$  is the damping matrix,  $n_d \times n_d$ ;  $[K]$  is the stiffness matrix,  $n_d \times n_d$ ;  $[L]$  is input matrix,  $n_d \times s$ . The mass matrix is positive definite (all its eigenvalues are positive), and the stiffness and damping matrices are positive semidefinite (all their eigenvalues are nonnegative).

### 3. Modelling of flexible cantilever plate system

Finite element analysis for  $10 \times 10$  m plate,  $\rho = 7800 \text{ kg/m}^3$ . Thickness is 0.001 m. This condition is illustrated in Fig. 6.

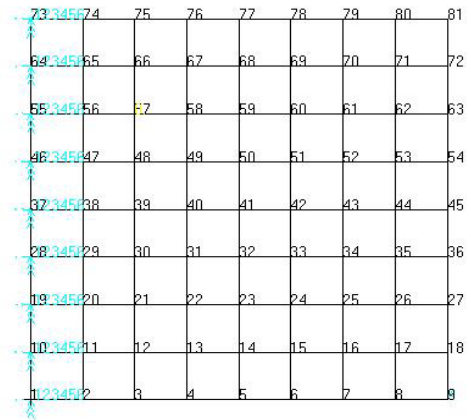


Fig. 6 Finite element model

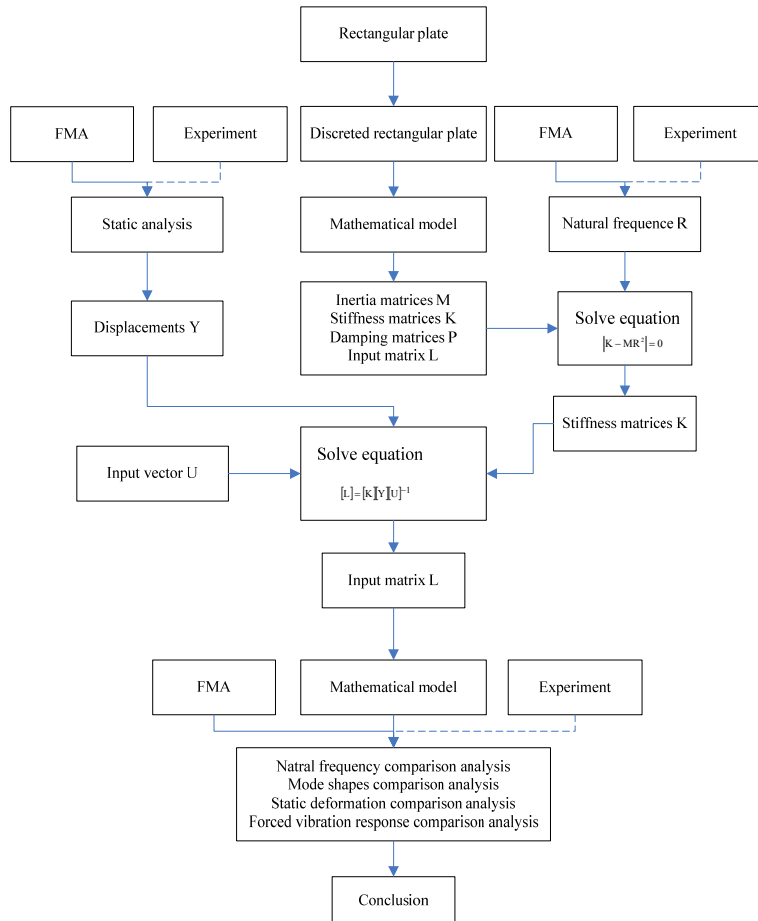


Fig. 7 Modelling method

Considering flowchart of modeling method (Fig. 7), we have  $[M]$ ,  $[P]$ ,  $[K]$ ,  $[L]$ .

#### 4. Validity of the new model

##### 4.1. Natural frequency comparison analysis

The results of natural frequency comparison analysis are shown in Table.

Table

Contrastive analysis results

Natural frequency	1	2	3	4	5
FEA result	0.17	0.41	1.06	1.35	1.54
New model of the natural frequency	0.23	0.44	1.12	1.41	1.97
Absolute error	0.06	0.03	0.06	0.06	0.43

Natural frequency	6	7	8	9
FEA result	2.71	3.19	3.32	3.70
New model of the natural frequency	2.82	2.94	3.29	3.61
Absolute error	0.11	0.11	0.03	0.09

##### 4.2. Forced vibration response analysis

When system is excited by a harmonic force, the vibration response of 39th node is shown by Fig. 8.

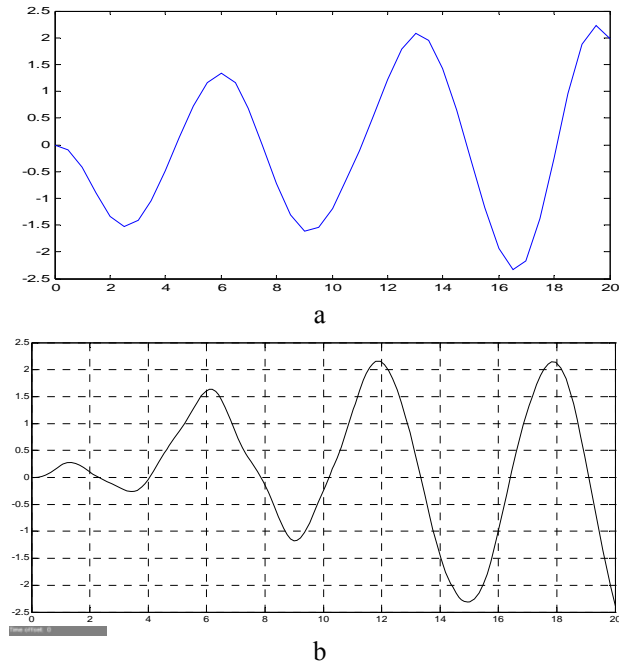


Fig. 8 Vibration response of flexible rectangular plate system (acting point of force is 39th node): a - result of FEM model; b - result of new model

##### 5. Adaptive iterative learning control design

Using the Lagrangian formulation, the equations of motion of a  $n$  degrees-of-freedom rectangular plate system may be expressed by

$$M(q_k(t))\ddot{q}_k(t) + C(q_k(t), \dot{q}_k(t))\dot{q}_k(t) + K(q_k(t)) = \tau_k(t) + d_k(t) \quad (33)$$

where  $t$  denotes the time and the nonnegative integer,  $k \in Z_+$  denotes the operation or iteration number. The signals  $q_k \in R^n$ ,  $\dot{q}_k \in R^n$  and  $\ddot{q}_k \in R^n$  are the node position, node velocity and node acceleration vectors, respectively, at the iteration  $k$ .  $M(q_k) \in R^{n \times n}$  is the inertia matrix,  $C(q_k, \dot{q}_k) \dot{q}_k \in R^{n \times n}$  is damping matrix.  $K(q_k) \in R^{n \times n}$  is the stiffness matrix.  $\tau_k \in R^n$  is the control input vector containing the forces to be applied at each node.  $d_k(t) \in R^n$  is the vector containing the unmodeled dynamics and other unknown external disturbances.

Assuming that the node positions and the node velocities are available for feedback, our objective is to design a control law  $\tau_k(t)$  guaranteeing the boundedness of  $q_k(t)$ ,  $\forall t \in [0, T]$  and  $\forall t \in Z_+$ , and the convergence of  $q_k(t)$  to the desired reference trajectory  $q_d(t)$  for all  $t \in [0, T]$  when  $k$  tends to infinity.

Throughout this paper, we will use the  $\ell_{pe}$  norm defined as follows

$$\|x(t)\|_{pe} \triangleq \begin{cases} \left( \int_0^t \|x(\tau)\|^p d\tau \right)^{1/p} & \text{if } p \in [0, \infty), \\ \sup_{0 \leq \tau \leq t} \|x(\tau)\| & \text{if } p = \infty \end{cases} \quad (34)$$

where  $\|x(t)\|$  denotes any norm of  $x$ , and  $t$  belongs to the finite interval  $[0, T]$ . We say that  $x \in \ell_{pe}$  when  $\|x(t)\|_{pe}$  exists (i.e., when  $\|x(t)\|_{pe}$  is finite).

We assume that all the system parameters are unknown and we make the following reasonable assumptions.

(A1) The reference trajectory and its first and second time-derivative, namely  $q_d(t)$ ,  $\dot{q}_d(t)$  and  $\ddot{q}_d(t)$ , as well as the disturbance  $d_k(t)$  are bounded  $\forall t \in [0, T]$  and  $\forall k \in Z_+$ .

(A2) The resetting condition is satisfied, i.e.,  $\dot{q}_d(0) - \dot{q}_k(0) = q_d(0) - q_k(0) = 0$ ,  $\forall k \in Z_+$ .

We will also need the following properties, which are common to rectangular plate system.

(P1)  $M(q_k) \in R^{n \times n}$  is symmetric, bounded, and positive definite.

(P2) The matrix  $x^T \dot{M}(q_k)x = 0$ ,  $\forall x \in R^n$ .

(P3)  $K(q_k) + C(q_k, \dot{q}_k)\dot{q}_k(t) = \Psi(q_k, \dot{q}_k)\xi(t)$ ,

where [5]  $\Psi(q_k, \dot{q}_k) \in R^{n \times (m-1)}$  is a known matrix and  $\xi(t) \in R^{m-1}$  is an unknown continuous vector over  $[0, T]$ .

(P4)  $\|C(q_k, \dot{q}_k)\| \leq k_c \|\dot{q}_k\|$  and  $\|K(q_k)\| < k_g$ ,  $\forall t \in [0, T]$  and  $\forall t \in Z_+$ , where  $k_c$  and  $k_g$  are unknown positive parameters.

Adaptive iterative learning controller design.

**Theorem 1.** Consider system (33) with properties (P1-P3) under the following control law

$$\tau_k(t) = K_p \tilde{q}_k(t) + K_D \dot{\tilde{q}}_k(t) + \phi(q_k, \dot{q}_k, \ddot{q}_k) \hat{\theta}_k(t) \quad (35)$$

with

$$\hat{\theta}_k(t) = \hat{\theta}_{k-1}(t) + \Gamma \phi^T(q_k, \dot{q}_k, \ddot{q}_k) \dot{\hat{q}}_k(t) \quad (36)$$

where  $\hat{\theta}_{-1}(t) = 0$ ,  $\tilde{q}_k(t) = q_d(t) - q_k(t)$  and  $\dot{\hat{q}}_k(t) = \dot{q}_d(t) - \dot{q}_k(t)$ . The matrix  $\phi(q_k, \dot{q}_k, \ddot{q}_k) \in R^{n \times m}$  is defined as  $\phi(q_k, \dot{q}_k, \ddot{q}_k) \triangleq [\Psi(q_k, \dot{q}_k) \text{sgn}(\dot{\hat{q}})]$ , where  $\text{sgn}(\dot{\hat{q}})$  is the vector obtained by applying the signum function to all elements of  $\dot{\hat{q}}$ . The matrices  $K_P \in R^{n \times n}$ ,  $K_D \in R^{n \times n}$  and  $\Gamma \in R^{m \times m}$  are symmetric positive definite. Let assumptions (A1-A2) be satisfied, then  $\tilde{q}_k(t) \in \ell_{\infty e}$ ,  $\dot{\tilde{q}}_k(t) \in \ell_{\infty e}$ ,  $\tau_k(t) \in \ell_{2e}$  for all  $k \in Z_+$  and  $\lim_{k \rightarrow \infty} \tilde{q}_k(t) = \lim_{k \rightarrow \infty} \dot{\tilde{q}}_k(t) = 0$ ,  $\forall t \in [0, T]$ .

The proof of this theorem is in three parts. The first part consists of taking a positive definite Lyapunov-like composite energy function, namely  $W_k$ , and show that this sequence is nonincreasing with respect to  $k$  and hence bounded if  $W_0$  is bounded. In the second part, we show that  $W_0(t)$  is bounded for all  $t \in [0, T]$ . Finally, in the third part, we show that  $\lim_{k \rightarrow \infty} \tilde{q}_k(t) = \lim_{k \rightarrow \infty} \dot{\tilde{q}}_k(t) = 0$ ,  $t \in [0, T]$ .

**Proof.** Part 1: Let us consider the following Lyapunov-like composite energy function

$$W_k(\dot{\hat{q}}_k(t), \tilde{q}_k(t), \tilde{\theta}_k(t)) = V_k(\dot{\hat{q}}_k(t), \tilde{q}_k(t)) + \frac{1}{2} \int_0^t \tilde{\theta}_k^T(\tau) \Gamma^{-1} \tilde{\theta}_k(\tau) d\tau \quad (37)$$

with  $\tilde{\theta}_k(t) = \theta(t) - \hat{\theta}_k(t)$ , where  $\theta(t) = [\xi^T(t) \ \beta]^T \in R^m$  and  $\hat{\theta}(t) = [\hat{\xi}^T(t) \ \hat{\beta}^T(t)]^T$  is the estimated value of  $\theta(t)$ . The unknown vector  $\xi(t)$  is defined in (P3) and the unknown parameter  $\beta$  is obtained according to (P1) and (A1) such that  $\|M(q_k)\ddot{q}_d - d_k\| \leq \beta$ ,  $\forall t \in [0, T]$  and  $\forall k \in Z_+$ .

The term  $V(\dot{\hat{q}}_k(t), \tilde{q}_k(t))$  in (37) is chosen as follows

$$V_k(\dot{\hat{q}}_k(t), \tilde{q}_k(t)) = \frac{1}{2} \dot{\hat{q}}_k^T M(q_k) \dot{\hat{q}}_k + \frac{1}{2} \dot{\hat{q}}_k^T K_P \dot{\hat{q}}_k \quad (38)$$

The difference of  $W_k$  is given by

$$\begin{aligned} \Delta W_k &= W_k - W_{k-1} = V_k - V_{k-1} + \\ &+ \frac{1}{2} \int_0^t (\tilde{\theta}_k^T \Gamma^{-1} \tilde{\theta}_k - \tilde{\theta}_{k-1}^T \Gamma^{-1} \tilde{\theta}_{k-1}) d\tau = \\ &= V_k - V_{k-1} - \frac{1}{2} \int_0^t (\bar{\theta}_k^T \Gamma^{-1} \bar{\theta}_k - \bar{\theta}_{k-1}^T \Gamma^{-1} \bar{\theta}_{k-1}) d\tau \end{aligned} \quad (39)$$

where  $\bar{\theta}_k = \hat{\theta}_k - \hat{\theta}_{k-1}$ . On the other hand, one can rewrite  $V_k$  as follows

$$V_k(\dot{\hat{q}}_k(t), \tilde{q}_k(t)) = V_k(\dot{\hat{q}}_k(0), \tilde{q}_k(0)) + \int_0^t \left( \dot{\hat{q}}_k^T M \ddot{\hat{q}}_k + \frac{1}{2} \dot{\hat{q}}_k^T \dot{M} \dot{\hat{q}}_k + \dot{\hat{q}}_k^T K_P \dot{\hat{q}}_k \right) d\tau \quad (40)$$

Now, using (33) and (P2, P3) we have

$$\begin{aligned} \dot{\hat{q}}_k^T M \ddot{\hat{q}}_k &= \dot{\hat{q}}_k^T M (\ddot{q}_d - \ddot{q}_k) = \\ &= \dot{\hat{q}}_k^T M \ddot{q}_d - \dot{\hat{q}}_k^T (-C\dot{q}_k - K + \tau_k + d_k) \end{aligned} \quad (41)$$

$$\frac{1}{2} \dot{\hat{q}}_k^T \dot{M} \dot{\hat{q}}_k = 0 \quad (42)$$

From known conditions we can have

$$\dot{\hat{q}}_k^T (M(q_k)\ddot{q}_d - d_k) \leq \|\dot{\hat{q}}_k\| \beta = \dot{\hat{q}}_k^T \beta \text{sgn}(\dot{\hat{q}}_k) \quad (43)$$

$$\left. \begin{aligned} \Psi(q_k, \dot{q}_k) \xi^T + \beta \text{sgn}(\dot{\hat{q}}_k) &= [\Psi(q_k, \dot{q}_k) \text{sgn}(\dot{\hat{q}}_k)] \\ [\xi^T \ \beta]^T &= \phi(q_k, \dot{q}_k, \dot{\hat{q}}_k) \theta \end{aligned} \right\} \quad (44)$$

Eq. (40) leads to

$$\begin{aligned} V_k(\dot{\hat{q}}_k(t), \tilde{q}_k(t)) &= V_k(\dot{\hat{q}}_k(0), \tilde{q}_k(0)) + \\ &+ \int_0^t \left[ \dot{\hat{q}}_k^T M \ddot{q}_d - \dot{\hat{q}}_k^T (-C\dot{q}_k - K + \tau_k + d_k) + \dot{\hat{q}}_k^T K_P \dot{\hat{q}}_k \right] d\tau = \\ &= V_k(\dot{\hat{q}}_k(0), \tilde{q}_k(0)) + \\ &+ \int_0^t \dot{\hat{q}}_k^T [M\ddot{q}_d + C\dot{q}_k + K - \tau_k - d_k + K_P \dot{\hat{q}}_k] d\tau \leq \\ &\leq V_k(\dot{\hat{q}}_k(0), \tilde{q}_k(0)) + \\ &+ \int_0^t \left[ \dot{\hat{q}}_k^T (\beta \text{sgn}(\dot{\hat{q}}_k) + \Psi(q_k, \dot{q}_k) \xi) + \dot{\hat{q}}_k^T (-\tau_k + K_P \dot{\hat{q}}_k) \right] d\tau \leq \\ &\leq V_k(\dot{\hat{q}}_k(0), \tilde{q}_k(0)) + \\ &+ \int_0^t \left[ \dot{\hat{q}}_k^T (\phi(q_k, \dot{q}_k, \dot{\hat{q}}_k)) \theta - \tau_k + K_P \dot{\hat{q}}_k \right] d\tau \end{aligned} \quad (45)$$

Now, substituting (35) in (45) we obtain

$$V_k(\dot{\hat{q}}_k(t), \tilde{q}_k(t)) \leq V_k(\dot{\hat{q}}_k(0), \tilde{q}_k(0)) + \int_0^t \left[ \dot{\hat{q}}_k^T (\phi(q_k, \dot{q}_k, \dot{\hat{q}}_k)) \tilde{\theta}_k - \tau_k + K_P \dot{\hat{q}}_k \right] d\tau \quad (46)$$

Using Eqs. (36), (46) and (A2), Eq. (39) leads to

$$\left. \begin{aligned} \Delta W_k &\leq -V_{k-1} - \\ &- \frac{1}{2} \int_0^t \dot{\hat{q}}_k^T (\phi(q_k, \dot{q}_k, \dot{\hat{q}}_k)) \Gamma \phi^T(q_k, \dot{q}_k, \dot{\hat{q}}_k) + 2K_D \dot{\hat{q}}_k d\tau \leq 0 \end{aligned} \right\} \quad (47)$$

Hence  $W_k$  is a nonincreasing sequence. Thus if  $W_0$  is bounded one can conclude that  $W_k$  is bounded. In Part 2 of the Proof we will show that  $W_0$  is bounded for all  $t \in [0, T]$ . Hence  $\tilde{q}_k(t)$ ,  $\dot{\tilde{q}}_k(t)$  and  $\int_0^t \tilde{\theta}_k^T(\tau) \Gamma^{-1} \tilde{\theta}_k(\tau) d\tau$  are bounded for all  $k \in Z_+$  and all  $t \in [0, T]$ . Since  $\theta(t)$  is continuous over  $[0, T]$ , the boundedness of

$\int_0^t \tilde{\theta}_k^T(\tau) \Gamma^{-1} \tilde{\theta}_k(\tau) d\tau$  implies the boundedness of  $\int_0^t \hat{\theta}_k^T(\tau) \Gamma^{-1} \hat{\theta}_k(\tau) d\tau$ . Consequently, one can conclude that  $\tau_k(t) \in \ell_{2e}$  for all  $k \in Z_+$ .

Part 2: Now, we will show that  $W_0(t)$  is bounded over the time interval  $[0, T]$ . In fact, considering (37) with  $k=0$ , the time-derivative of  $W_0$  can be bounded as follows

$$\dot{W}_0 \leq \tilde{q}_0^T \left( \phi(q_0, \dot{q}_0, \ddot{q}_0) \tilde{\theta}_0 - K_D \dot{\tilde{q}}_0 \right) + \frac{1}{2} \tilde{\theta}_0^T \Gamma^{-1} \tilde{\theta}_0 \quad (48)$$

Since  $\hat{\theta}_{-1}(t) = 0$ , one has

$$\hat{\theta}_0(t) = \Gamma \phi^T(q_0, \dot{q}_0, \ddot{q}_0) \tilde{q}_0(t). \text{ Hence}$$

$$\dot{W}_0 \leq -\dot{\tilde{q}}_0^T K_D \dot{\tilde{q}}_0 + \left( \hat{\theta}_0^T + \frac{1}{2} \tilde{\theta}_0^T \right) \Gamma^{-1} \tilde{\theta}_0 \quad (49)$$

Using Young's inequality, we have

$$\theta^T \Gamma^{-1} \tilde{\theta}_0 \leq \kappa \|\Gamma^{-1} \tilde{\theta}_0\|^2 + \frac{1}{4\kappa} \|\theta\|^2 \quad (50)$$

for any  $\kappa > 0$ . Hence

$$\dot{W}_0 \leq -\rho_1 \|\dot{\tilde{q}}_0\|^2 - \rho_2 \|\tilde{\theta}_0\|^2 + \frac{1}{4\kappa} \|\theta\|^2 \quad (51)$$

with  $\rho_1 = \lambda_{\min}(K_D)$ ,  $\rho_2 = \frac{1}{2} \lambda_{\min}(\Gamma^{-1}) - \kappa \lambda_{\max}^2(\Gamma^{-1})$  and  $0 < \kappa \leq \lambda_{\min}(\Gamma^{-1}) / 2 \lambda_{\max}^2(\Gamma^{-1})$ , where  $\lambda_{\min}(\cdot)$  ( $\lambda_{\max}(\cdot)$ ) denotes the minimal (maximal) eigenvalue of  $(\cdot)$ . Since  $\theta$  is continuous over  $[0, T]$ , it is clear that it is bounded over  $[0, T]$ , i.e.,  $\|\theta\|_{\infty} \leq \theta_{\max}$ . Hence, one can conclude from (51) that  $\dot{W}_0(t) \leq \theta_{\max}^2 / (4\kappa)$ , which implies that  $W_0(t)$  is uniformly continuous and thus bounded over  $[0, T]$ .

Part 3: Note that  $W_k$  can be written as follows

$$W_k = W_0 + \sum_{j=1}^k \Delta W_j. \text{ Hence, using (37), one has}$$

$$\begin{aligned} W_k &\leq W_0 - \sum_{j=1}^k V_{j-1} \leq \\ &\leq W_0 - \frac{1}{2} \sum_{j=1}^k \tilde{q}_{j-1}^T K_P \tilde{q}_{j-1} - \frac{1}{2} \sum_{j=1}^k \tilde{q}_{j-1}^T M(q_{j-1}) \dot{\tilde{q}}_{j-1} \end{aligned} \quad (52)$$

Which implies that

$$\sum_{j=1}^k \tilde{q}_{j-1}^T K_P \tilde{q}_{j-1} + \sum_{j=1}^k \tilde{q}_{j-1}^T M(q_{j-1}) \dot{\tilde{q}}_{j-1} \leq 2(W_0 - W_k) \leq 2W_0 \quad (53)$$

Hence  $\lim_{k \rightarrow \infty} \tilde{q}_k(t) = \lim_{k \rightarrow \infty} \dot{\tilde{q}}_k(t) = 0, \forall t \in [0, T]$ .

Note that under properties (P1-P3) the control law (35)-(36) involves  $m$  iterative parameters, where  $m$  is

generally larger than the number of degrees-of-freedom  $n$ . It also requires the knowledge of the matrix  $\Psi(q_k, \dot{q}_k)$ . However, by using (P4) instead of (P3), the knowledge of the matrix  $\Psi(q_k, \dot{q}_k)$  is not required anymore and the number of iterative parameters is reduced to two as stated in the following theorem.

## 6. Simulation example

Considering  $[M], [P], [K], [L]$  and letting

$$M(q) = [M], C(q, \dot{q}) = [P], K(q) = [K][Y], \tau = [L][F], \Phi(q, \dot{q}_r, \ddot{q}, \ddot{q}_r) = [L]$$

$$\Gamma = \begin{bmatrix} 400 & 400 & 400 & 400 & 400 & 400 & 400 & 400 & 400 \\ & & & & & & & & \\ & & & & & & & & \\ & & & & & & & & \\ & & & & & & & & \\ & & & & & & & & \\ & & & & & & & & \\ & & & & & & & & \\ & & & & & & & & \end{bmatrix}$$

$$K_p = \begin{bmatrix} 200 & 200 & 200 & 200 & 200 & 200 & 200 & 200 & 200 \\ & & & & & & & & \\ & & & & & & & & \\ & & & & & & & & \\ & & & & & & & & \\ & & & & & & & & \\ & & & & & & & & \\ & & & & & & & & \\ & & & & & & & & \end{bmatrix}$$

$$K_D = \begin{bmatrix} 200 & 200 & 200 & 200 & 200 & 200 & 200 & 200 & 200 \\ & & & & & & & & \\ & & & & & & & & \\ & & & & & & & & \\ & & & & & & & & \\ & & & & & & & & \\ & & & & & & & & \\ & & & & & & & & \\ & & & & & & & & \end{bmatrix}$$

The desired joint trajectory is given by

$$\begin{aligned} q1\_d &= \sin(2\pi t); & q2\_d &= \cos(2\pi t); & q3\_d &= \sin(2\pi t); \\ q4\_d &= \cos(2\pi t); & q5\_d &= \sin(2\pi t); \\ q6\_d &= \cos(2\pi t); & q7\_d &= \sin(2\pi t); & q8\_d &= \cos(2\pi t); \\ q9\_d &= \sin(2\pi t); \end{aligned}$$

The displacements and velocities are chosen as

$$x = [\dot{y}_1 \ \dot{y}_1 \ \dot{y}_2 \ \dot{y}_2 \ \dot{y}_3 \ \dot{y}_3 \ \dot{y}_4 \ \dot{y}_4 \ \dot{y}_5 \ \dot{y}_5 \ \dot{y}_6 \ \dot{y}_6 \ \dot{y}_7 \ \dot{y}_7 \ \dot{y}_8 \ \dot{y}_8 \ \dot{y}_9 \ \dot{y}_9]$$

The initial displacements and velocities are chosen as

$$x_0 = [0; 1; 1; 0; 0; 1; 1; 0; 0; 1; 1; 0; 0; 1; 1; 0; 0; 0]$$

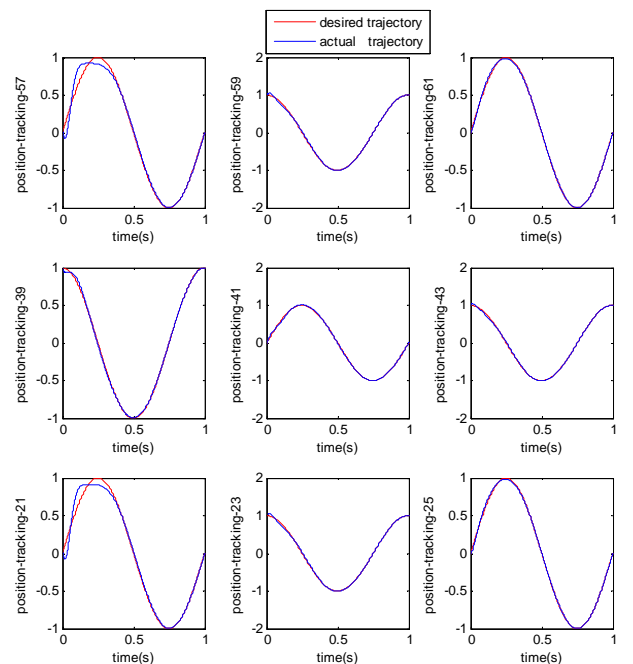


Fig. 9 Position tracking error of 57th node, 59th node, 61th node, 39th node, 41th node, 43th node, 21th node, 23th node, 25th node respectively

Using control laws (35), (36), Fig.9 shows Position tracking error of 57th node, 59th node, 61th node, 39th node, 41th node, 43th node, 21th node, 23th node, 25th node respectively.

## 7. Conclusions

Adaptive iterative learning MIMO control strategy for the active vibration control of a flexible rectangular plate structure was developed. It was shown that the new modeling method is a kind of development with respect to the plant modeling theory of current control theory. It provides theoretical basis for low order controller design of high order plant with unknown parameters, adaptive controller design and intelligent controller design. It also brings about great convenience for engineering design. The first nine natural frequencies, mode shapes, static analysis and forced vibration response analysis of the flexible rectangular plate structure considered in this study were predicted accurately and compared by the FEM method and new modeling method and thus, the validity of the proposed new model was confirmed. An adaptive iterative learning MIMO controller was then employed to attenuate the unwanted vibration of a rectangular flexible plate system simulated using the MATLAB/Simulink platform. The simulation results demonstrate the effectiveness of the proposed control technique. Future works will be directed towards the development of an experimental rig to validate the theoretical results obtained in the study.

## Acknowledgment

The work was supported by the Funding for Outstanding Doctoral Dissertation in NUAA (BCXJ10-01), Funding of Jiangsu Innovation Program for Graduate Education (CX10B\_089Z), NUAA Research Funding ( No. NS20100060).

## References

1. **Hu, Q.; Ma, G.; C. Li.** 2004. Active vibration control of a flexible plate structure using LMI-based  $H_\infty$  output feedback control law, Proceedings of the 5<sup>th</sup> World Congress on Intelligent Control and Automation, China, 738-742.
2. **Kar, I.N.; Miyakura, T.; Seto, K.** 2000. Bending and torsional vibration control of a flexible plate structure using  $H_\infty$  based robust control law, IEEE Trans. Control Syst. Technol. 8(3): 545-553.
3. **Xianmin, Z.; Changjian, Sh.; Erdman, A.G.** 2002. Active vibration controller design and comparison study of flexible linkage mechanism systems, J. Mech. Mach. Theory 37: 985-997.
4. **Bakšys, B.; Ramanauskytė, K.; Povilionis, A.B.** 2009. Vibratory manipulation of elastically unconstrained part on a horizontal plane, Mechanika 1(75): 36-41.

5. **Craig, J.J.** 1986. Introduction to robotics: mechanics and control. Reading, MA: Addison-Wesley.

Jingyu Yang, Guoping Chen

## ADAPTYVUS PRIARTĖJIMO BŪDU APSIMOKANTIS LENKIAMOS STAČIAKAMPĖS PLOKŠTĖS VIBRACIJŲ VALDYMAS

### R e z i u m ė

Šiame straipsnyje naudojant valdymo teoriją nagrinėjama lenkiamos stačiakampės plokštės aktyvi svyravimų kontrolė. Lenkiamos stačiakampės plokštės sistema yra modeliuojama naudojant baigtinių elementų metodą ir naują modeliavimo būdą. Tam naudotas erdvinis modelis sudarant erdvinio judesio lygtis, kurios yra efektyviai naudojamos analizuojant sistemą ir kuriant valdymo algoritmą. Naujo sudaryto modelio skaičiavimo rezultatai naudojami lyginant plokštės savuosius svyravimus, jų tipą, atliekant statistinę analizę ir reakciją į priverstinius svyravimus su rezultatais gautais atlikus skaičiavimus baigtinių elementų metodu. Patikrinus, adaptyvusis pasikartojantis MIMO kontroleris pritaikytas plokštės dinamikai tirti MATLAB/Simulink programa. Imitavimo rezultatai parodė efektyvų svyravimų slopinimą, kuri galima gauti naudojant adaptyvųjį MIMO kontrolerį.

Jingyu Yang, Guoping Chen

## ADAPTIVE ITERATIVE LEARNING CONTROL FOR VIBRATION OF FLEXURAL RECTANGULAR PLATE

### S u m m a r y

In this paper, we developed an approach for active vibration control of flexible rectangular plate structures using control theory. The flexible rectangular plate system is firstly modeled and simulated via a finite element method; and secondly, a new type of modeling method, and the state-space model are involved in the development of the equation of motion in state-space, which is efficiently used for the analysis of the system and design of control laws with a modern control framework. Then, the validity of the obtained new model is investigated by comparing the plate natural frequencies, mode shapes, statical analysis and forced vibration response analysis predicted by the finite element model with the calculated values obtained from new model. After validating the model, adaptive iterative learning MIMO controller is applied to the plate dynamics via the MATLAB/Simulink platform. The simulation results clearly demonstrate an effective vibration suppression capability that can be achieved using adaptive iterative learning MIMO controller.

Received March 15, 2011

Accepted October 12, 2011